Charge transfer and optical phonon mixing in few-layer graphene chemically doped with sulfuric acid

WeiJie Zhao, PingHeng Tan,* Jun Zhang, and Jian Liu
State Key Laboratory for Superlattices and Microstructures, Institute of Semiconductors, Chinese Academy of Sciences, Beijing 100083, China

(Received 4 March 2010; revised manuscript received 9 October 2010; published 16 December 2010)

Chemical doping is expected to substantially increase the density of free charge carriers by charge transfer and modify the Fermi level and screening effect of doped materials. Here, along with Raman identification of 3 and 4 graphene layers by a 633-nm laser excitation, we investigated charge transfer and optical phonon mixing in few layer graphenes in detail by utilizing sulfuric acid as an electron-acceptor dopant. Sulfuric acid molecules are found to be only physically adsorbed on the surface layers of graphenes without intercalations. The top and bottom layers of bilayer graphene can be intentionally doped differently by concentrated sulfuric acid. The difference of the hole doping between the top and bottom layers results in phonon mixing of symmetric and antisymmetric modes in bilayer graphene. The Raman frequency evolution with the doping level is in agreement with recent *ab initio* density-functional theory calculations [P. Gava, M. Lazzeri, A. M. Saitta, and F. Mauri, Phys. Rev. B **80**, 155422 (2009)]. Chemical doping by adsorption-induced charge transfer offers a way to study the electronic and vibrational behaviors of few layer graphenes at high-carrier concentration.

DOI: 10.1103/PhysRevB.82.245423 PACS number(s): 78.30.Na, 63.22.Rc, 78.66.Tr, 81.05.ue

I. INTRODUCTION

Graphene, the latest carbon allotrope discovered in 2004,[1] has attracted intensively scientific interest owing to its distinctive properties. Two-dimensional structure of nanoscale and extremely high carrier mobilities at room temperature make it a promising candidate for future nanoelectronics.[1–7] Raman spectroscopy has been proved an efficient way for identifying graphene layers,[7–9] probing the electronic structure of graphenes,[7,10,11] and providing information of defects,[12,13] stacking order,[7,14,15] and doping.[11,16–19] The most prominent Raman features in graphene,[7] as well as other carbon materials,[20,21] are the D band, G band, and the 2D band (so-called G′ band). The D band at around 1350 cm^{-1} is due to the breathing modes of sp^2 atoms and requires a defect for its activation.[22,23] The G band at around 1580 cm^{-1} is a doubly degenerate optical phonon mode at the Brillouin-zone center.[24] The 2D band is the second order of the D band, and its line shape has been widely used to distinguish the number of graphene layers.[7–9,13]

For monolayer graphene, the Fermi level locates at the Dirac point and can be shifted by varying doping charge concentration.[1–4] The E_{2g} phonon energy at the Brillouin-zone center exhibits a logarithmic singularity when the Fermi energy shift (E_F) from the Dirac point is half of the phonon energy.[16,25–27] For an intrinsic bilayer graphene (BLG), the zone-center mode splits into a symmetric mode (in-phase displacement of the atoms in the two layers) and an antisymmetric mode (out-of-phase displacement of the atoms in the two layers).[28–30] The symmetric mode is Raman active while the antisymmetric mode is infrared active.[28–30] Therefore there is only a single G peak for intrinsic BLGs.[7–16,18,19] If the bilayer graphene is doped symmetrically, meaning no difference of the doping charge concentrations of top layer (n_t) and bottom layer (n_b), the symmetric and antisymmetric modes can not mix. However, if the doping charge concentrations of the two layers are different ($n_t \neq n_b$), the inversion symmetry in the BLG is broken, and a gap between conduction and valence bands is opened up.[29,31–35] The symmetric and antisymmetric modes are no longer eigenstates in comparison with the intrinsic BLG and strongly coupled with each other.[28–35] The Raman spectrum was predicted to show two G peaks with different frequency shifts and intensities.[28–30] Recent experiments confirmed the prediction in the asymmetrically doped BLGs.[36–38] In the case of asymmetrically doped 3L and 4L graphenes, the evolution of the G band of 3L and 4L graphenes with increasing doping, respectively, shows similar behavior to that of 1L and 2L graphenes.[38] The splitting of the G band is observed in the 4L graphene with asymmetry doping but not in the 3L graphene owing to distinct electron-phonon coupling for phonons of different symmetry.[38]

Not only the electrical doping via applying gate voltage[36,37] but also chemical doping via atoms/molecules deposition on the top and/or bottom layers can break the inversion symmetry of BLGs.[29,38,39] In comparison with electrical doping,[36,37] chemical doping enables us to manipulate the electrostatic environment of graphene layers.[29,38,39] In this case, one can manipulate the charge concentrations between top and bottom layers of BLGs to reveal how the electrostatic environment induces an optical phonon mixing phenomenon. When the graphene layers are doped by adsorption/intercalation of Br and I atoms[39] or F atoms,[38] the symmetrical and asymmetrical doping can be obtain. Furthermore, the doping status is not stable when the graphene layers are under ambient conditions.[38,40] In this work, we report that the top and bottom layers of BLG can be intentionally doped differently by concentrated sulfuric acid. The difference of the hole doping between the top and bottom layers breaks the inversion symmetry in BLGs and results in phonon mixing of symmetric and antisymmetric G modes. Chemical doping by concentrated sulfuric acid gives us an

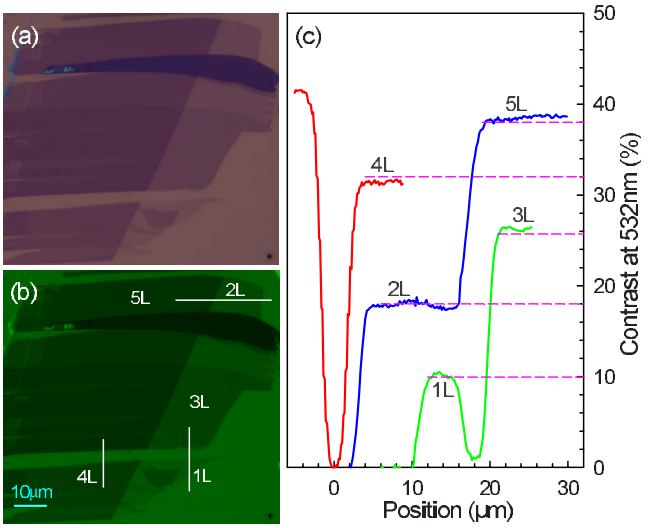

FIG. 1. (Color online) Optical image of a pristine 1–5L graphene sample using (a) white light and (b) a bandpass filter at 532 nm with a full width at half maximum of 9 nm. (c) Experimental data (solid line) of the optical contrast at 532 nm obtained from three solid lines in (b). The discrepancy between experimental and theoretical (dashed lines) data are lower than 5%.

opportunity to study electron-phonon coupling, screening effect and band-gap formation of BLGs in the case of high doping level.

II. EXPERIMENTAL

Graphene samples were obtained by micromechanical cleavage of natural graphite on the surface of a Si wafer chip with 293-nm-thick SiO_2 on the top.[1,2] 18 mole (18 M) concentration sulfuric acid (H_2SO_4) was used and diluted with distilled water to lower mole concentration (14 M, 10 M, and 6 M). Raman measurements were performed in a backscattering geometry at room temperature using a Jobin-Yvon HR800 Raman system, which is equipped with liquid nitrogen cooled charge coupled device. The output power of 633 nm He-Ne laser was 1 mW in order to avoid sample heating.[41] *In situ* Raman measurements were done when graphene samples were immersed in different acids using a 600 lines/mm grating and a 100× long working distance objective lens (NA=0.75). Furthermore, the 2L graphene samples were washed by distilled water flow for a few seconds, dried in electronic drying cabinet, and reinserted into the spectrometer. These Raman measurements were done using a 1200 lines/mm grating and a 100× objective lens (NA=0.90). The Raman mapping was measured by duoscan system of HR800. The spectral resolution of 600 lines/mm and 1200 lines/mm gratings is 1.2 cm^{-1} and 0.6 cm^{-1} for HR800 system, respectively, due to its long focal length of 800 mm. All Raman peaks are fitted with Lorentzian line shapes.

III. RESULTS AND DISCUSSION

The graphene layer can be identified by the optical contrast,[1,38,42,43] atomic force microscopy image and the line

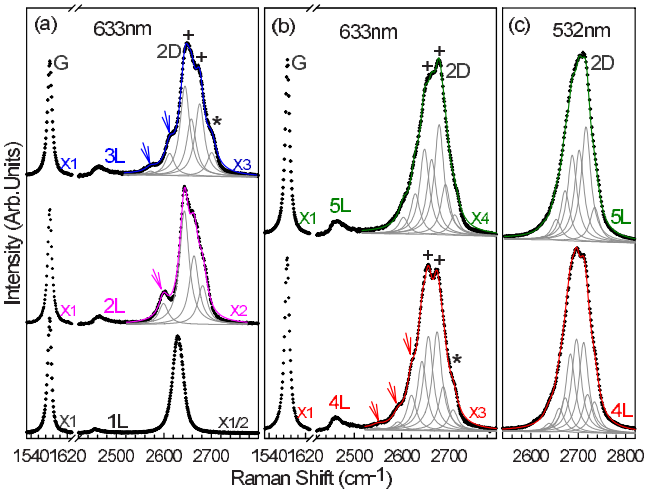

FIG. 2. (Color online) Raman spectra (dotted curves) of G and 2D peaks of pristine (a) 1–3L graphenes excited by a 633 nm laser and those of 4L and 5L graphenes excited by (b) the 633 nm laser and by (c) a 532 nm laser, respectively. The 2D peaks were fitted by Lorentzian line shapes (gray peaks). The solid lines with colors are the fitted results. The arrows indicate the weak shoulders at the low energy side of the 2D peaks for 2–4L graphenes. The crosses shows the strongest components of the 2D peaks for 3–5L graphenes. The stars labels the weak shoulders at the high energy side of the 2D peaks for 3–4L graphenes.

shape of the 2D peak.[7–9,15] The optical images of a 1–5L graphene sample are shown in Figs. 1(a) and 1(b) obtained using white light and a bandpass filter at 532 nm [full width at half maximum (FWHM) of 9 nm], respectively. Figure 1(c) shows the experimental optical contrast (defined as 1-RG/RS, where RG and RS are the reflected light intensities from the SiO_2/Si substrate with and without graphenes, respectively) at 532 nm of the 1–5L graphenes. Compared with the theoretical results using optical constants of graphene layers suggested by Bruna *et al.*,[38,43] 1–5L graphenes can be clearly identified.

The 633 and 532 nm lasers are widely used in the Raman measurements for various carbon materials.[7,13,15,20,44] Figure 2 shows Raman spectra of 1–3L graphenes by a 633 nm laser and 4–5L graphenes by 633 and 532 nm lasers. All G peaks are at around 1580 cm^{-1}, and can be fitted with a single Lorentzian line shape. Monolayer graphene has a single 2D peak at 2629.7 cm^{-1}. The 2D band of 2L graphene is fitted with four Lorentzian peaks.[7] The 2D bands of 3–5L graphenes are more complex and in principle consist of 9, 16, and 25 Lorentzian peaks,[45] respectively. However, because of the possible degeneracy and overlapping of these peak components, the number of observed components is much less than the theoretical one. The 2D band of the 4L graphene by 633 nm excitation show more distinct spectral features than that by 532 nm excitation. However, for a 5L graphene, no clear distinct features can be identified both for 532 nm and 633 nm excitations, so the 2D band of 5L graphene is simply fitted with seven peaks as shown in Figs. 2(b) and 2(c). Here, we only focus on Raman identification of 1–4L graphenes. The pristine bernal-stacking graphene samples with the same layer number show identical spectral

TABLE I. Peak position (cm^{-1}) of the G peak and the fitting components of the 2D peaks for 1–4L graphenes excited by a 633 nm laser. The value (cm^{-1}) in parentheses is FWHM of the G peak. *w*, *m*, and *s* stand for weak, middle, and strong intensity for the 2D components, respectively.

	G	$2D_1$	$2D_2$	$2D_3$	$2D_4$	$2D_5$	$2D_6$	$2D_7$	$2D_8$
1L	1582				2630				
	(10.0)				*s*				
2L	1581			2599	2643	2664	2682		
	(11.5)			*m*	*s*	*m*	*m*		
3L	1581	2572	2612	2638	2648	2660	2675	2699	
	(12.0)	*w*	*m*	*m*	*s*	*m*	*s*	*m*	
4L	1580	2549	2592	2620	2642	2656	2674	2688	2708
	(12.8)	*w*	*w*	*m*	*m*	*s*	*s*	*m*	*m*

features. Because the different components of 2D bands may exhibit different resonant behaviors with laser excitations,[10] it is very important to choose an appropriate laser wavelength to identify graphene layers from Raman spectra. As shown in Figs. 2(a) and 2(b) by arrows, crosses and stars, five and six 2D components can be clearly identified in the Raman spectra of 3L and 4L graphenes excited by the 633 nm excitation, respectively. However, to obtain good fits, seven and eight components are, respectively, required for the 2D bands of 3L and 4L graphenes if the peak width of all components are kept as a fixed constant (24 cm^{-1}) (Ref. 10) in the fitting process. The fitting results of the 2D bands for 1–4L graphenes are summarized in Table I. The main peak position of the 2D peak in 1–4L graphenes upshifts with increasing of graphene layer. To identify 3L and 4L bernal-stacking graphenes by Raman scattering, it is better to use a 633 nm laser as excitation and to verify peak position and number of shoulders at the lower energy side and the intensity ratio of the strongest two components of their 2D bands, as indicated by arrows and crosses in Figs. 2(a) and 2(b). To reveal the spectral fingerprint of 3–4L graphenes, a Raman system with a high resolution better than 1.0 cm^{-1} is necessary. Along with the reported peculiar spectral feature of 1–2L graphenes,[7,9] Raman spectroscopy can be used to clearly identified 1–4L bernal-stacking graphenes with a 633 nm excitation associated with their optical contrast.

When 1–4L graphene samples were dipped into 18 M H_2SO_4, their G bands exhibit a significant change in peak position, as shown in the Fig. 3(a). The G bands of the 1L and 2L graphenes in 18 M H_2SO_4 acid show an identical spectral feature to that of graphenes adsorbed and intercalated by Br_2 vapors,[39] such as peak position and width. The G peak shifts to 1623.8 cm^{-1} and 1613.4 cm^{-1} for 1L and 2L graphenes, respectively. The great upshift in G bands for 1–2L graphenes with respect to 1582 cm^{-1} of graphite indicates charge transfer from the physically adsorbed or intercalated H_2SO_4 molecules. The charge transfer from graphene to H_2SO_4 creates hole doping in graphene,[46] as a well-known electron-acceptor dopant in graphite compounds.[47] Indeed, when 1L graphene was dipped into 10 M H_2SO_4, the 2D peak upshifts about 10 cm^{-1}, as shown in Fig. 3(b), which is a typical characteristic of hole doping in graphene layers.[11,19] The Fermi Level is shifted largely due to hole doping.[11,16–19,39] We find that the saturation time of the chemical doping of graphenes by H_2SO_4 is very fast, within 1 min. We did not observed any change for more than 1 h. The absence of D band, before and after doping, suggests that the samples have a high crystal quality and the concentrated sulfuric acid treatment did not induce structural damage to graphenes.

The single G peak at 1613.4 cm^{-1} for BLG demonstrates that it was doped symmetrically, otherwise, the inversion symmetry in the bilayer graphene induced by different doping charge concentrations of its two layers will be broken, which makes the single G peak in pristine BLGs change into two Raman peaks.[28–30,36,37] This indicates that the H_2SO_4 molecules can diffuse entirely along the interface between the bottom layer and substrate. However, in contrast to the 1L and 2L graphenes, the 3L and 4L graphenes in 18 M H_2SO_4 acid show a quite different spectral feature from that doped by Br_2 vapors,[39] and their G peaks appear with a doublet structure (G^+ for upper peak and G^- for lower peak). The G^+ peak shifts to 1608.2 cm^{-1} and 1604.3 cm^{-1} for 3L

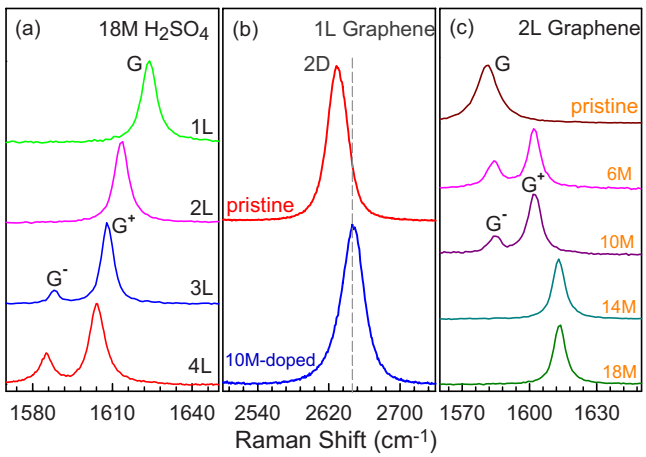

FIG. 3. (Color online) (a) *In situ* Raman spectra of the G peak of 1–4L graphene samples dipped into 18 mole (18 M) concentration of sulfuric acid. (b) The 2D band of pristine 1L graphene and that doped by 10 M concentration of sulfuric acids. (c) *In situ* Raman spectra of the G peak of the BLG doped by different mole concentrations (18 M, 14 M, 10 M, and 6 M) of sulfuric acids and a pristine BLG as a reference.

TABLE II. Peak position, width (FWHM), and intensity ratio of G^+ and G^- components of the G peak for 1–4L graphenes doped by 18 M sulfuric acids.

	1L	2L	3L	4L
Position (cm^{-1})			1588.1	1585.0
	1623.8	1613.4	1608.2	1604.3
Width (cm^{-1})			3.8	5.7
	6.8	6.4	5.3	6.8
I_{G+}/I_{G-}			8.6	3.4

and 4L graphenes, respectively. All the peak parameters are summarized in Table II. The G (or G^+) peak downshifts to lower frequency with increasing the layer number. The singlet G peak for 4L graphene doped by Br_2 vapors indicates that Br_2 intercalates a 4L graphene into two 2L graphenes.[39] In contrast, the doublet G peak for 4L graphene in Fig. 3(a) indicates that sulfuric acid molecules only physically adsorb on the surface layers and no intercalation happens. The surface layers were doped more heavily than the interior, due to screening.[39,48] Consequently, two G peaks were observed, as the case in stage 4 graphite intercalation compounds.[47] The G^+ and G^- peaks were assigned to phonon mixing of the symmetric and antisymmetric modes in surface and interior layers.[37,39] The similar doublet G peak for 3L graphene in Fig. 3(a) also confirms the above proposition. Indeed, the G peaks of 1–4L graphenes in Fig. 3(a) are very similar with that of 1–4L graphenes exposed to iodine vapor, where the mechanism of chemical doping is the adsorption of iodine on the surface graphene layers.[39]

The G peaks of 1L and 2L graphenes in 18 M H_2SO_4 are identical to that of graphenes exposed to Br_2 vapors, while the corresponding 3L and 4L graphenes show a similar G-band feature to graphenes exposed to I_2 vapors, although the chemical doping mechanisms for Br_2 and I_2 vapors on graphene are quite different.[39] To further clarify the chemical doping mechanism of H_2SO_4 on graphenes, different treatments are performed on a BLG sample. Figure 3(c) shows Raman spectra of the BLG dipped into different concentrations of sulfuric acid. The doublet feature of G peak appears in the Raman spectra of 6 and 10 M H_2SO_4 doped BLGs, and a single G peak was observed in 14 and 18 M H_2SO_4 doped BLGs. This indicates sulfuric acid molecules cannot diffuse efficiently between the bottom layer and substrate in 6 and 10 M H_2SO_4 owing to the decrease in sulfuric acid concentration. The asymmetric hole doping, due to different amount of H_2SO_4 molecules physically adsorbed on the top layer and bottom layer, breaks the inverse symmetry in BLG, which makes the symmetric mode and antisymmetric mode mix with each other. As a result, two G peaks were observed as predictions.[28–30]

To continually change the carrier concentration on the top and bottom layers of BLGs, several washing processes were performed step by step on a BLG sample, whose optical image was shown in Fig. 4(a). The BLG sample dipped in 18 M H_2SO_4 was taken out and washed by distilled water flow for a few seconds, and then dried for Raman measurement at the same position of spot A [see Fig. 4(a)]. Figure 4(b) shows

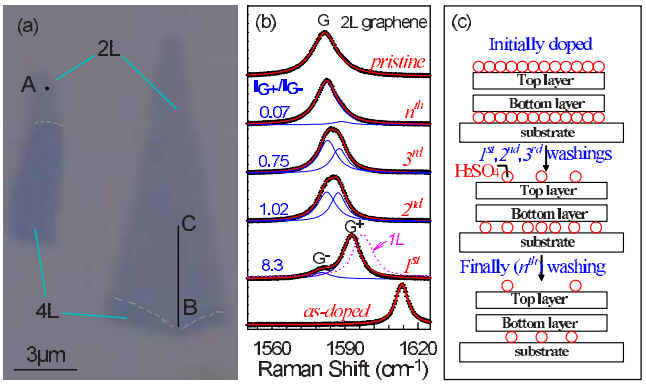

FIG. 4. (Color online) (a) An optical image of a sample contained BLGs and 4L graphenes. The scale bar is 3 μm. The boundary of 4L graphenes close to BLGs is indicated by dashed lines. (b) Raman spectra of the G peak of the pristine and as-doped BLG sample at spot A, and those after first, second, third, and *n*th washings by distilled water. The G peak (dotted line) of an as-doped 1L graphene after first washing is also shown as a reference. (c) Schematic of the concentration distribution of doping charges on top and bottom layers of a BLG doped by 18 M sulfuric acid, after first, second, third, and *n*th washings by distilled water.

typical G peaks of doped BLGs after different washing processes (first, second, third and *n*th) and a pristine BLG. After washing, the doublet feature of the G band was observed again, and the G peak decreases from 1613 to 1589 $cm^{-1}(G^+)$. A 1L graphene sample dipped in 18 M H_2SO_4 was also used as a reference to verify the change in carrier concentration in the washing process. After the first washing, the G band of 1L graphene decreases from 1624 to 1598 cm^{-1}, as indicated in Fig. 4(b) by a dashed line. Note that 1598 cm^{-1} is much lower than that (1613 cm^{-1}) of 2L graphene doped by 18 M H_2SO_4. This suggests that not only the H_2SO_4 molecules adsorbed on the top surface of 1L graphene but also some of them on the bottom surface were washed away. Therefore, the acid molecules adsorbed on the top layer of BLG were more easily washed away than the ones between the bottom layer and substrate. The different doping hole concentration of the two layers in washed BLGs gave rise to a doublet feature of the G band.

The G peaks in Figs. 3(c) and 4(b) were fitted by Lorentzian line shapes and the G peak parameters are summarized in Tables III and IV, respectively. The intensity ratio of I_{G+}/I_{G-} significantly changes with the washing process (0.03–6.0 from first to *n*th washings), which directly reveals that the doping level is decreased with increasing washing times. The FWHM of G^- increases with the decreasing of the doping level while G^+ shows a broader feature, which is close to that of the G peak in pristine BLGs. The width evolution seems in contradiction to the common result of the decrease in peak width with increasing doping level, however, the peak position and intensity evolution of the G^+ and G^- peaks with doping level agree well with previous studies.[36–38] A simple coupled-mode description had been applied to interpret phonon mixing behavior of the gated BLGs.[30,37] When the total doping hole density $n(=n_t+n_b)$ (sign of n, n_t and n_b: positive for hole doping and negative for electron doping) is very small (far below 10^{13} cm^{-2}),

TABLE III. Peak position, width (FWHM), and intensity ratio of G^+ and G^- components of the G peak for pristine BLG and that doped by different mole concentrations (18 M, 14 M, 10 M, and 6 M) of sulfuric acids.

	Pristine	6 M	10 M	14 M	18 M
Position (cm^{-1})	1581.8	1584.1	1584.6		
		1602.0	1602.3	1613.1	1613.4
Width (cm^{-1})	11.5	7.3	6.2		
		6.4	7.0	6.4	6.4
I_{G+}/I_{G-}		2.1	4.1		

only a single broadening G peak (G^-) at low frequency exists, due to the symmetric mode coupling with direct interband electron-hole pairs.[30] With increase in n up to about 5×10^{12} cm^{-2},[37] the FWHM of G^- decreases and an extra weak peak (G^+) appears at the high frequency. With the continuous increase in n, the intensity of the G^+ peak increases while that of the G^- peak decreases.[30,37] At greatly high n, there is only a strong G^+ peak as the case of BLGs doped by 18 M H_2SO_4. However, a quantitative explanation of the Raman spectra of chemically doped BLGs is still a challenge because of complex electrostatic environment of BLGs,[28–30,38] such as inhomogeneous doping and substrate effect. In this work, the substrate doping to the graphene can be negligible in comparison with the chemical doping. Indeed, the G peak of pristine BLGs here is about 1581–1582 cm^{-1} with a good Lorentzian line shape and a typical width (FWHM) of 11–12 cm^{-1}.

We performed a line scan of Raman spectra of the H_2SO_4-doped BLG along the line B-C as shown in Fig. 4(a) after its second washing. The increment of the line scan is 0.6 μm. Due to acid molecules just physically adsorbed on top graphene layer of BLGs, they can be easily removed by washing, and n_t will be far below 10^{13} cm^{-2}. n_b is mainly determined by the concentration of acid molecules intercalated between the substrate and bottom layer of the BLG as discussed above about the G peak of pristine BLGs. After washing, there is a doping charge distribution of n_b in the bottom layer of BLGs. All the G peaks are analyzed with two Lorentzians, G^+ and G^-. The ratio I_{G+}/I_{G-} varies from 0.6 to 6.4 and peak positions of G^+ and G^- strongly depend on the measured sample spot, as shown in Figs. 5(a) and 5(b). We utilize recent theoretical results, which shows that the ratio I_{G+}/I_{G-} strongly depends on n_t while the frequency shifts have a much weaker dependence,[29] to model our experimental data. After washing, the n_t is expected to be very low in comparison with the high n_b and can be considered as a constant. Therefore, we fit the obtained I_{G+}/I_{G-} values [Squares in Fig. 5(a)] to the theoretical curves of $n_t=0.2$, 0.3, and 0.4×10^{13} cm^{-2}, and obtain a set of total doping hole density n at each sample spot. Then, the frequency shift in G^+ and G^- depending on n is shown in Fig. 5(b). For gated graphenes[11,16–19,36,37] at $E_F=0$, the variation in the reported G peak position is several wavenumber, from 1581 to 1585 cm^{-1}. When the graphenes are chemically doped by H_2SO_4 and washed by distilled water, the environment between the graphene layers and adsorbed sulfuric acid molecules becomes more complex. Therefore, the trend of peak shift dependent on the charge concentration qualitatively agrees with the theoretical predicts.[29] If we execute the same procedures for the data in Table IV, we found that the data deviate far away from the theoretical curve of $n_t=0.3\times10^{13}$ cm^{-2} because the different washing processes would significantly change the doping charge concentrations of top layer (n_t), so a fixed n_t can not be applied to model all the data in Table IV.

To exam how about the detail doping behavior of BLGs by H_2SO_4, Raman map was further performed on the large sample in Fig. 4(a). Figure 6(a) shows the Raman map of total area intensity (I_{G+}/I_{G-}) of the G peak. The 4L graphene at the lower part of the sample can be clearly distinguished. Although the BLG sample looks homogenous from the optical image in Fig. 4(a), the total intensity of the G peak exhibits a dependence on the doping charge concentration and reaches to a maximum value at center region. Figures 6(b) and 6(c) show the intensity ratio I_{G+}/I_{G-} and frequency difference ($P_{G+}-P_{G-}$) mappings of G^+ and G^- components of the G peak, respectively. The two maps agree well with each other and each map shows a maximum value near the center

TABLE IV. Peak position, width (FWHM), and intensity ratio of G^+ and G^- components of the G peak for a pristine BLG and the doped BLGs by 18 M sulfuric acids sequentially following with first, second, third, and nth washings by distilled water.

	Pristine	nth	Third	Second	First
Position (cm^{-1})	1581.8	1582.5	1583.0	1582.5	1580.3
		1589.0	1587.8	1587.2	1592.3
Width (cm^{-1})	11.5	10.2	8.8	9.0	9.1
		6.5	7.4	7.6	8.0
I_{G+}/I_{G-}		0.05	0.58	0.85	6.0

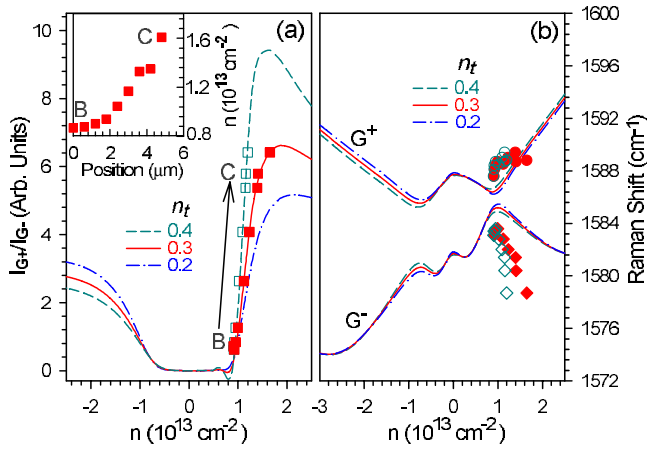

FIG. 5. (Color online) Data of line scan along B-C on the doped BLGs in Fig. 4(a) after the second washing process. (a) The measured intensity ratio I_{G+}/I_{G-} was modelled by theoretical results (Ref. 29) with n_t of 0.2×10^{13} cm^{-2}, 0.3×10^{13} cm^{-2}, and 0.4×10^{13} cm^{-2}, respectively, to get the corresponding total doping charge concentration n. Inset shows the obtained charge concentration dependent on the position of laser spots. (b) The frequency of G^+ and G^- as a function of n determined from the ratio I_{G+}/I_{G-} in (a). Solid symbols represent experimental data modelled by the theoretical curve (Ref. 29) of the ratio I_{G+}/I_{G-} for n_t=0.3 $\times10^{13}$ cm^{-2}, and open symbols represent experimental data corresponding to n_t=0.4$\times10^{13}$ cm^{-2}.

of the sample. I_{G+}/I_{G-} and $P_{G+}-P_{G-}$ provide a fingerprint of the doping charge concentration on the bottom graphene layer of BLGs close to the substrate if the doping charge concentration is assumed to be homogenous on the top layer, as discussed above. Indeed, Raman measurement shows that the doping level is homogenous for the as-doped graphene sample by H_2SO_4.[49] The acid molecules adsorbed on the top layer can be easily washed away while those intercalated between the bottom layer and substrate could be only removed by the diffusion via the concentration difference between inner and outer regions. Thus, the concentration of acid molecules intercalated between the bottom layer and substrate decreases from the sample center to edge, as indicated in Figs. 6(b) and 6(c), due to the washing of distilled water. When the sample was washed for many times, the unevenness of doping level from sample center to edge becomes very small.

The G peaks of Raman spectra in Fig. 6 were analyzed to obtain detailed peak parameters of the doped BLGs. Unlike the gated graphenes,[11,16–19,36,37] it is difficult to determine the carrier concentration in the chemically doped graphenes. However, as shown in Fig. 5(a), the intensity ratio I_{G+}/I_{G-} is very sensitive to the doping level in BLGs and can be serviced as a signature of doping level in asymmetrically doped bilayer graphenes.[29] Figures 7(a) and 7(b) summarize the peak width and width ratio of G^- and G^+ components dependent on I_{G+}/I_{G-}. For the G^- peak, the width is about 12 cm^{-1} in pristine BLG. When the BLG starts to be doped to I_{G+}/I_{G-}=0.6, the width will decrease to 9 cm^{-1} statistically. As increasing the doping level, the width will increase up to 13 cm^{-1} until the G^- peak vanishes at a high doping level. For the G^+ peak, the width will increase from about 5 cm^{-1} at low doping level to about 8 cm^{-1} when I_{G+}/I_{G-}=0.6. When the doping level increases up to a maximum value, the G^+ position reaches up to 1613 cm^{-1} as the case in Fig. 3(c), the G^+ width will decrease down to about 6.5 cm^{-1}. The observed behavior of peak width depending on the doping level is not in agreement with theoretical calculation,[29,30] where the width of G^- continually decreases with increasing doping level, while for the G^+ peak there is a maximum width when n is close to 0.8×10^{13} cm^{-2}, corresponding to I_{G+}/I_{G-} of 0.6. The intrinsic theoretical behavior of peak width on the doping level may be overlapped by the broadening effect from adsorbed acid molecules and uniform doping in doped BLGs. However, the width ratio of G^- and G^+ dependent on I_{G+}/I_{G-} shows the similar trend as theoretical results.[29] Lower the I_{G+}/I_{G-}, larger the width ratio between G^- and G^+.

Figure 8 shows how the doping level affects the peak positions of G^+ and G^-. The G^- peak is more sensitive to the doping status in the present case than the G^+ peak. The frequency difference between G^+ and G^- shows more clear dependence on the doping level of BLGs. A similar behavior of chemical doping on graphene by CHF_3 plasma treatment was reported by Bruna *et al.*[38] where the 85% of the total charge carriers is assumed to be confined in the top layer. We can not provide a detailed fitting of experimental result in Fig. 8 to the theoretical one here because all the data from each spot on the sample after washing by distilled water flow would make the status away from a ideal case although the doping of as-doped graphene sample by H_2SO_4 is homogenous. However, using the obtained n_t of 0.3×10^{13} cm^{-2},

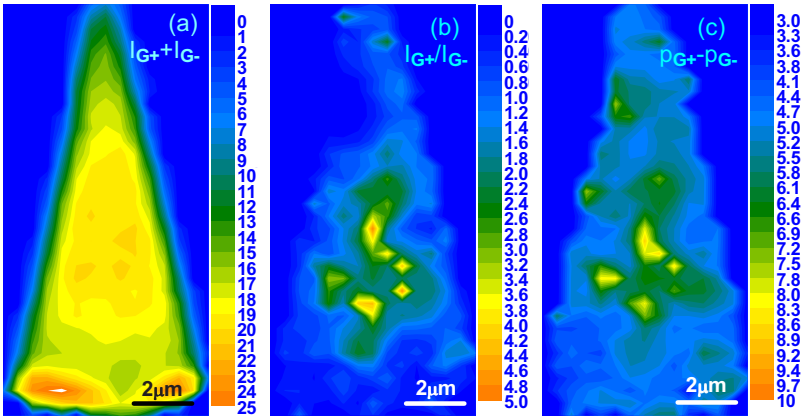

FIG. 6. (Color online) (a) Raman map of total intensity ($I_{G+}+I_{G-}$) of the G peak for the doped BLGs in Fig. 4(a) after the second washing process. (b) Raman map of the corresponding intensity ratio of I_{G+}/I_{G-}. (c) Raman map of the corresponding peak shift ($P_{G+}-P_{G-}$) between G^+ and G^- components of the G peak.

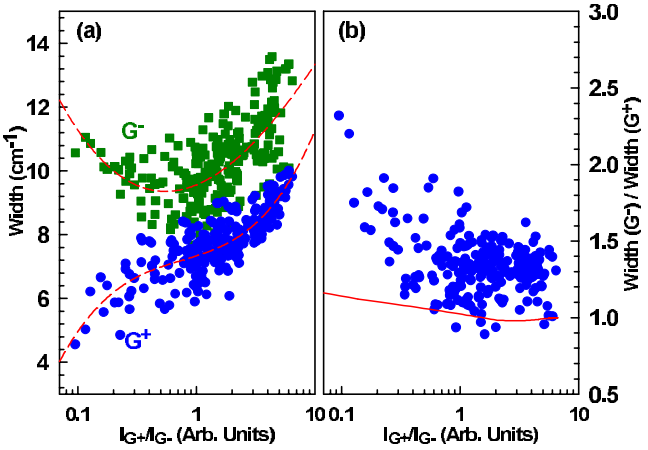

FIG. 7. (Color online) (a) Peak width of the G peak in Raman map in Fig. 6 as a function of the intensity ratio I_{G+}/I_{G-}. The dashed lines are guides to the eyes. (b) Dependence of the width ratio of G^- and G^+ components on the intensity ratio I_{G+}/I_{G-}. The solid line represents the theoretical curve (Ref. 29).

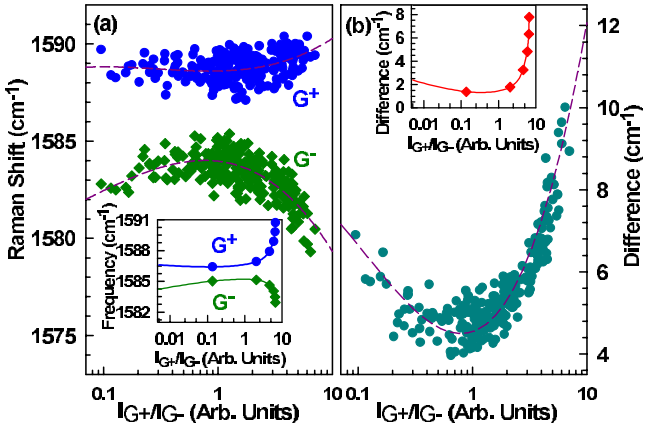

FIG. 8. (Color online) Peak position (a) and frequency difference (b) of G^+ and G^- components in Raman map in Fig. 6 as a function of the intensity ratio I_{G+}/I_{G-}. Insets show the corresponding theoretical curve when $n_t=0.3\times10^{13}$ cm^{-2} by Gava *et al.* (Ref. 29). The dashed lines are guides to the eyes.

the trend of peak position and frequency difference of G^+ and G^- as a function of their intensity ratio I_{G+}/I_{G-} agrees with Gava's theoretical work,[29] as shown in the insets to Figs. 8(a) and 8(b). This demonstrates that the frequency difference and intensity ratio of G^+ and G^- components can be treated as fingerprints for the doping level of the asymmetrically doped BLGs.

At last, it should be addressed that chemically doped BLGs by sulfuric acid are very stable in air when they were taken out of concentrated sulfuric acid. Raman frequency of the G peak almost keeps constant in air at room temperature for more than four months. On contrary, the doping charge concentration of graphene layers doped by Br_2 will decrease very fast when the graphenes are exposed to air.[40] This indicates that physical adsorption of sulfuric acid molecules on graphene's surface layers is very stable in air. Sulfuric acid molecules could be a stable donor for the purpose of chemical doping graphene layers both in fundamental researches and device applications.

IV. CONCLUSION

In conclusion, charge transfer of few layer graphenes resulting from chemical doping of sulfuric acids is studied by Raman spectroscopy. The doping mechanism of sulfuric acids is not intercalation, but adsorption of sulfuric acid molecules on the surface layers of graphenes, which makes the top and bottom layer of bilayer graphenes can be intentionally doped differently. Asymmetric hole doping breaks the inverse symmetry in BLGs, and results in a mixing of symmetric and antisymmetric modes and a splitting (G^+ and G^-) of the G peak. The evolution of frequency shift, difference between G^+ and G^-, peak width and intensity ratio are investigated in detail at different level of carrier concentration. It shows that peak position of G^+ and G^- and frequency difference between G^+ and G^- as a function of the intensity ratio of I_{G+}/I_{G-} qualitatively agree with recently calculations.[29] Sulfuric acid molecules can be expected as a stable electron-acceptor dopant for graphenes to study the physical properties of few layer graphenes at different doping levels.

ACKNOWLEDGMENTS

This work was supported by the National Natural Science Foundation of China under Grants No. 10934007 and No. 10874177, and the special funds for the Major State Basic Research under Contract No. 2009CB929300 of China.

*phtan@semi.ac.cn

[1] K. S. Novoselov, A. K. Geim, S. V. Morozov, D. Jiang, Y. Zhang, S. V. Dubonos, I. V. Grigorieva, and A. A. Firsov, Science **306**, 666 (2004).

[2] K. S. Novoselov, A. K. Geim, S. V. Morozov, D. Jiang, M. I. Katsnelson, I. V. Grigorieva, S. V. Dubonos, and A. A. Firsov, Nature (London) **438**, 197 (2005).

[3] Y. Zhang, Y.-W. Tan, H. L. Stormer, and P. Kim, Nature (London) **438**, 201 (2005).

[4] J. B. Oostinga, H. B. Heersche, X. L. liu, A. F. Morpurgo, and L. M. K. Vandersypen, Nature Mater. **7**, 151 (2008).

[5] S. V. Morozov, K. S. Novoselov, M. I. Katsnelson, F. Schedin, D. C. Elias, J. A. Jaszczak, and A. K. Geim, Phys. Rev. Lett. **100**, 016602 (2008).

[6] X. Du, I. Skachko, A. Barker, and E. Y. Andrei, Nat. Nanotechnol. **3**, 491 (2008).

[7] A. C. Ferrari, J. C. Meyer, V. Scardaci, C. Casiraghi, M. Lazzeri, F. Mauri, S. Piscanec, D. Jiang, K. S. Novoselov, S. Roth, and A. K. Geim, Phys. Rev. Lett. **97**, 187401 (2006).

[8] A. Gupta, G. Chen, P. Joshi, S. Tadigadapa, and P. C. Eklund,

Nano Lett. **6**, 2667 (2006).
[9] D. Graf, F. Molitor, K. Ensslin, C. Stampfer, A. Jungen, C. Hierold, and L. Wirtz, Nano Lett. **7**, 238 (2007).
[10] L. M. Malard, J. Nilsson, D. C. Elias, J. C. Brant, F. Plentz, E. S. Alves, A. H. Castro Neto, and M. A. Pimenta, Phys. Rev. B **76**, 201401(R) (2007).
[11] A. Das, B. Chakraborty, S. Piscanec, S. Pisana, A. K. Sood, and A. C. Ferrari, Phys. Rev. B **79**, 155417 (2009).
[12] C. Casiraghi, A. Hartschuh, H. Qian, S. Piscanec, C. Georgi, A. Fasoli, K. S. Novoselov, D. M. Basko, and A. C. Ferrari, Nano Lett. **9**, 1433 (2009).
[13] A. C. Ferrari, Solid State Commun. **143**, 47 (2007).
[14] Z. Ni, Y. Wang, T. Yu, Y. You, and Z. Shen, Phys. Rev. B **77**, 235403 (2008).
[15] P. Poncharal, A. Ayari, T. Michel, and J.-L. Sauvajol, Phys. Rev. B **78**, 113407 (2008).
[16] S. Pisana, M. Lazzeri, C. Casiraghi, K. S. Novoselov, A. K. Geim, A. C. Ferrari, and F. Mauri, Nature Mater. **6**, 198 (2007).
[17] J. Yan, Y. Zhang, P. Kim, and A. Pinczuk, Phys. Rev. Lett. **98**, 166802 (2007).
[18] J. Yan, E. A. Henriksen, P. Kim, and A. Pinczuk, Phys. Rev. Lett. **101**, 136804 (2008).
[19] A. Das, S. Pisana, B. Chakraborty, S. Piscanec, S. K. Saha, U. V. Waghmare, K. S. Novoselov, H. R. Krishnamurthy, A. K. Geim, A. C. Ferrari, and A. K. Sood, Nat. Nanotechnol. **3**, 210 (2008).
[20] P. H. Tan, C. Y. Hu, J. Dong, W. Shen, and B. Zhang, Phys. Rev. B **64**, 214301 (2001).
[21] A. Jorio, R. Saito, G. Dresselhaus, and M. S. Dresselhaus, Philos. Trans. R. Soc. London, Ser. A, **362**, 2311 (2004); C. Thomsen, S. Reich, and J. Maultzsch, *ibid.* **362**, 2337 (2004); S. Reich and C. Thomsen, *ibid.* **362**, 2269 (2004); P. H. Tan, S. Dimovski, and Y. Gogotsi, *ibid.* **362**, 2289 (2004).
[22] A. C. Ferrari and J. Robertson, Phys. Rev. B **61**, 14095 (2000).
[23] C. Thomsen and S. Reich, Phys. Rev. Lett. **85**, 5214 (2000).
[24] F. Tuinstra and J. L. Koenig, J. Chem. Phys. **53**, 1126 (1970).
[25] A. H. Castro Neto and F. Guinea, Phys. Rev. B **75**, 045404 (2007).
[26] T. Ando, J. Phys. Soc. Jpn. **75**, 124701 (2006).
[27] M. Lazzeri and F. Mauri, Phys. Rev. Lett. **97**, 266407 (2006).
[28] T. Ando, J. Phys. Soc. Jpn. **76**, 104711 (2007).
[29] P. Gava, M. Lazzeri, A. M. Saitta, and F. Mauri, Phys. Rev. B **80**, 155422 (2009).
[30] T. Ando and M. Koshino, J. Phys. Soc. Jpn. **78**, 034709 (2009).
[31] P. Gava, M. Lazzeri, A. M. Saitta, and F. Mauri, Phys. Rev. B **79**, 165431 (2009).
[32] Y. Zhang T. T. Tang, C. Girit1, Z. Hao, M. C. Martin, A. Zettl, M. F. Crommie, Y. R. Shen, and F. Wang, Nature (London) **459**, 820 (2009).
[33] E. V. Castro, K. S. Novoselov, S. V. Morozov, N. M. R. Peres, J. M. B. Lopes dos Santos, J. Nilsson, F. Guinea, A. K. Geim, and A. H. Castro Neto, Phys. Rev. Lett. **99**, 216802 (2007).
[34] E. McCann and V. I. Falko, Phys. Rev. Lett. **96**, 086805 (2006).
[35] E. McCann, Phys. Rev. B **74**, 161403(R) (2006).
[36] L. M. Malard, D. C. Elias, E. S. Alves, and M. A. Pimenta, Phys. Rev. Lett. **101**, 257401 (2008).
[37] J. Yan, T. Villarson, E. A. Henriksen, P. Kim, and A. Pinczuk, Phys. Rev. B **80**, 241417(R) (2009).
[38] M. Bruna and S. Borini, Phys. Rev. B **81**, 125421 (2010).
[39] N. Jung, N. Kim, S. Jockusch, N. J. Turro, P. Kim, and L. Brus, Nano Lett. **9**, 4133 (2009).
[40] W. J. Zhao, P. H. Tan, and J. Zhang (unpublished).
[41] P. H. Tan, Y. M. Deng, Q. Zhao, and W. C. Cheng, Appl. Phys. Lett. **74**, 1818 (1999).
[42] Z. H. Ni, H. M. Wang, J. Kasim, H. M. Fan, T. Yu, Y. H. Wu, Y. P. Feng, and Z. X. Shen, Nano Lett. **7**, 2758 (2007).
[43] M. Bruna and S. Borini, Appl. Phys. Lett. **94**, 031901 (2009).
[44] P. H. Tan, L. An, L. Q. Liu, Z. X. Guo, R. Czerw, D. L. Carroll, P. M. Ajayan, N. Zhang, and H. L. Guo, Phys. Rev. B **66**, 245410 (2002).
[45] J. S. Park, A. Reina, R. Saito, J. Kong, G. Dresselhaus, and M. S. Dresselhaus, Carbon **47**, 1303 (2009).
[46] N. A. Cordero and J. A. Alonso, Nanotechnology **18**, 485705 (2007).
[47] M. S. Dresselhaus and G. Dresselhaus, Adv. Phys. **30**, 139 (1981).
[48] F. Guinea, Phys. Rev. B **75**, 235433 (2007).
[49] See supplementary material at http://link.aps.org/supplemental/10.1103/PhysRevB.82.245423 for Raman map of the total area intensity and the intensity ratio I_{G+}/I_{G-} of the G band of as-doped BLGs by 18 M H_2SO_4 before and after the washing procedure.